Rapid determination of earthquake magnitude using GPS for tsunami warning systems

Geoffrey Blewitt,[1] Corné Kreemer,[1] William C. Hammond,[1] Hans-Peter Plag,[1] Seth Stein,[2] and Emile Okal[2]

The 26 December 2004 Sumatra earthquake (M_w 9.2–9.3) generated the most deadly tsunami in history. Yet within the first hour, the true danger of a major oceanwide tsunami was not indicated by seismic magnitude estimates, which were far too low (M_w 8.0–8.5). This problem relates to the inherent saturation of early seismic-wave methods. Here we show that the earthquake's true size and tsunami potential can be determined using Global Positioning System (GPS) data up to only 15 min after earthquake initiation, by tracking the mean displacement of the Earth's surface associated with the arrival of seismic waves. Within minutes, displacements of >10 mm are detectable as far away as India, consistent with results using weeks of data after the event. These displacements imply M_w 9.0 ± 0.1, indicating a high tsunami potential. This suggests existing GPS infrastructure could be developed into an effective component of tsunami warning systems.

1. Introduction

Even far away from an earthquake epicenter, tsunami warning is a race against time. Within three hours after the great Sumatra earthquake of 26 December 2004 (origin time, T_0 = 00:58:53 UTC), a tsunami crossed the ocean at the speed of a jet aircraft and devastated the coasts of Thailand, Sri Lanka, and India. Because of this high speed, developing systems to provide timely warnings is a major challenge. The first crucial hour after the Sumatra earthquake illustrates the challenge [*Kerr*, 2005] faced by the Pacific Tsunami Warning Center (PTWC).

[1]Nevada Bureau of Mines and Geology, and Seismological Laboratory, University of Nevada, Reno, Nevada, USA.

[2]Department of Geological Sciences, Northwestern University, Evanston, Illinois, USA

With no ocean-based sensor system deployed in the Indian Ocean, PTWC was entirely dependent on seismological data to assess the situation. PTWC's first bulletin at 01:10:00 UTC (T_0+11 min) estimated its magnitude at 8.0, using an algorithm known as M_{wp}, which integrates the low-frequency content of seismic body waves, but is ill-adapted to earthquake sources of unusually long duration. This low estimate indicated essentially zero risk of a major oceanwide tsunami [*Menke and Levin*, 2005]. About 1 hr after the earthquake, using surface wave data, the estimate was raised to moment magnitude M_w 8.5, for which an oceanwide tsunami would be likely (though not likely create far-field destruction). Within 5 hr, the Harvard Centroid Moment Tensor (CMT) Project adapted its computation to use longer period (300-s versus the standard 135-s) surface waves to infer M_w 9.0, for which the tsunami risk would be very high. Even this method could not entirely accommodate the long duration (>500 s) of the source [*Iishi et al.*, 2005]. Days later, analysis using the Earth's longest period normal modes [*Stein and Okal*, 2005; *Park et al.*, 2005] found even larger M_w values of 9.2–9.3, which have been confirmed by revised CMT analysis [*Tsai et al.*, 2005].

Tsunamis are gravitational oscillations of the ocean, in this case generated by the rapid displacement of the ocean floor at the trench associated with fault slip during the earthquake. Hence the tsunami potential of an earthquake is related to its seismic moment $M_0 = \mu s A$ (where μ is rigidity, s is the mean slip on the fault, and A is the area of the fault). M_0 is often reported in terms of the moment magnitude M_w [*Hanks and Kanamori*, 1979]. Thus, of the various earthquake magnitudes that can be computed from seismic observations, M_w is the most appropriate to assess tsunami potential, but is the most difficult to determine quickly because most seismological techniques are sensitive to the shorter period components. Algorithms have been developed [*Okal*

and Talandier, 1989; *Tsuboi et al.*, 1995; *Weinstein and Okal*, 2005] to rapidly assess M_w for purposes of tsunami warning. However, the longest period surface waves (typically 400–500 s) may underestimate M_w for great earthquakes whose duration equals or exceeds those periods. This was the case for the 2004 Sumatra event.

2. Approach

An alternative approach is to use the measured permanent co-seismic displacements of the Earth's surface. These directly relate to the mechanism that generates tsunamis, and are well-suited for estimation using GPS. The potential of GPS data to contribute to tsunami warning is suggested by remarkable observations [*Banerjee et al.*, 2005; *Vigny et al.*, 2005] showing that the Sumatra earthquake produced permanent, static displacements >10 mm as far away as India (~2000 km from the epicenter), with detectable displacements (few mm) beyond 3000 km. Displacement data have long been used [*Blewitt et al.*, 1993; *Bock et al.*, 1993] to determine the seismic moment M_0 and hence the moment magnitude M_w of earthquakes. When using GPS, M_0 is often called the "static moment", which should equal the seismic moment if the fault ruptured entirely seismically. GPS estimates of the Sumatra earthquake's static moment correspond to M_w 9.0–9.2 [*Banerjee et al.*, 2005; *Vigny et al.*, 2005; *Kreemer et al.*, 2006], consistent with longest period seismology [*Stein and Okal*, 2005; *Park et al.*, 2005]. Hence if GPS data had been analyzed rapidly and accurately, the resulting static displacements could have quickly indicated the earthquake's true size and tsunami potential.

3. Analysis

To test the feasibility of this approach, we used GPS data of the International GNSS Service (IGS) global network to estimate the static displacements using only data up to T_0+15 min, and then compared these to long-term estimates using weeks of data after the earthquake. We then assessed how well these static displacements constrain M_w starting only with knowledge of the earthquake epicenter from seismology. To make this test realistic, our model assumed the preliminary epicenter (3.4°N, 95.7° E) initially distributed by the PTWC at 01:10 UTC = T_0+11 min (S. Weinstein, personal communication, 2005).

We analyzed data from 38 GPS stations up to 7500 km from the epicenter. Only two stations qualify as "near field" (<1 rupture length of the epicenter), where motions >10 mm are expected: (i) SAMP at Medan, Indonesia (300 km), and (ii) NTUS at Singapore (900 km). The eight mid-field stations (1600–3000 km distance) are expected to show smaller but detectable displacements of a few mm. The remaining 28 far-field stations (3500–7500 km) are too distant to provide useful rapid constraints on the earthquake, but provide a far-field reference frame in which to monitor the displacements of closer stations, and provide wide-aperture data to determine the satellite orbits and Earth rotation parameters. This minimal network geometry, particularly in the near field, provides a challenging test of the method.

Using GIPSY-OASIS II software, GPS data at 30-s epochs were reduced to a time series of station longitude, latitude and height, by a customized procedure that simulates a real-time analysis situation, unlike traditional methods [e.g., *Vigny et al.*, 2005]. The analysis only used 24 hr of data until T_0+20.4 min (01:19:17 UTC = 01:19:30 GPS), applying a strategy that only uses information that could be available in real time. Simultaneously estimated parameters included the Earth's pole position and drift rate, the Earth's rate of rotation, satellite orbit state vectors (initialized using the Broadcast Ephemeris acquired prior to the earthquake), stochastic solar radiation pressure on the satellites, satellite and station clocks at every 30-s epoch, random-walk variation in zenith tropospheric delay and gradients over each station, carrier phase biases and cycle slips, and GPS station positions. Station positions were estimated in two categories: the 28 far-field station positions were estimated as constants over the 24-hr period, and the 10 near- to mid-field station positions were estimated independently at every 30-s epoch. The inversion was performed by a square-root information filter, which is well-suited to real-time operation [*Bierman*, 1977]. The actual processing time for a 38-station network is ~15% of real time on an ordinary 1-cpu PC running Linux, thus posing no fundamental problem for real-time implementation.

In addition, the station coordinate time series were calibrated to mitigate carrier phase multipath error, which approximately repeats every sidereal day

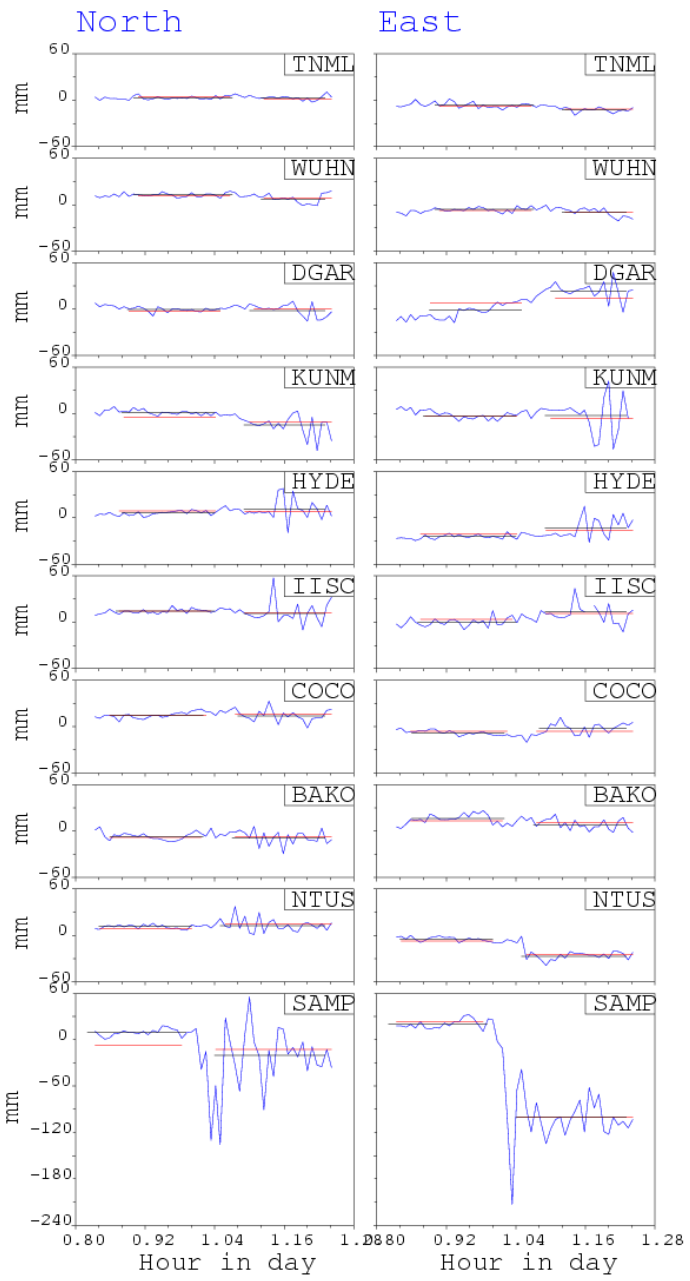

Figure 1. Time series of positions (blue) estimated every 30 s for stations ranked (bottom to top) by distance from the epicenter. Two types of fit to the data are shown before and after earthquake initiation. The black lines indicate mean positions estimated empirically from the time series, and the red lines are from the best-fitting earthquake model.

[*Genrich and Bock*, 1992; *Choi et al.*, 2004]. This calibration was computed using a position-based sidereal filter, by stacking the 30-s epoch coordinate time series from the previous 4 days, shifting each series by 4 min per day.

4. Results

The resulting time series of station positions (Fig. 1) clearly shows that most of the permanent, static displacement occurs within a few minutes of the first detectable arrival of seismic waves, accompanied by strong shaking that initially overshoots the final static position. We devised a simple algorithm that differences the mean position before and after the seismic waves arrive. First, let us define for each station the "nominal first arrival time" T_f to be conservatively early, as that of a wave traveling in a straight line at 11 km/s. Positions are then averaged from T_f -10 min to T_f, and also from T_f +3 min to the deadline, defined at T_0+15 min. The 3-min gap between these windows is designed to avoid sampling the initial step in position. For tsunami warning an early deadline is preferred, provided the estimate is sufficiently precise. Therefore, to assess the suitability of a 15-min deadline, we also tested 10-min and 20-min deadlines.

To test the precision of our estimated rapid displacements, we compared them with published displacements [*Banerjee et al.*, 2005; *Vigny et al.*, 2005; *Kreemer et al.*, 2006] based on weeks of data following the event, and computed RMS differences over all 20 horizontal displacement coordinates. As expected, the RMS difference progressively decreases as the deadline is extended. At 15 min the RMS is ~7 mm, and at 20 min the results change negligibly. As a general rule, 7-mm precision corresponds to the expected magnitude of displacements as far as ~2 rupture lengths away from the rupture; so a GPS network of this scale should be suitably sensitive to the size of the earthquake.

We then used the static displacements to infer an earthquake model and M_w given only knowledge that is expected to be available within minutes of the earthquake. We used the rapidly available seismic epicenter, whose location was assumed to indicate a thrust faulting event on the Sumatra-Andaman subduction zone. Based on this information, we assumed the earthquake ruptures away from the

epicenter in either direction along the known trench geometry [*Gudmundsson and Sambridge*, 1998].

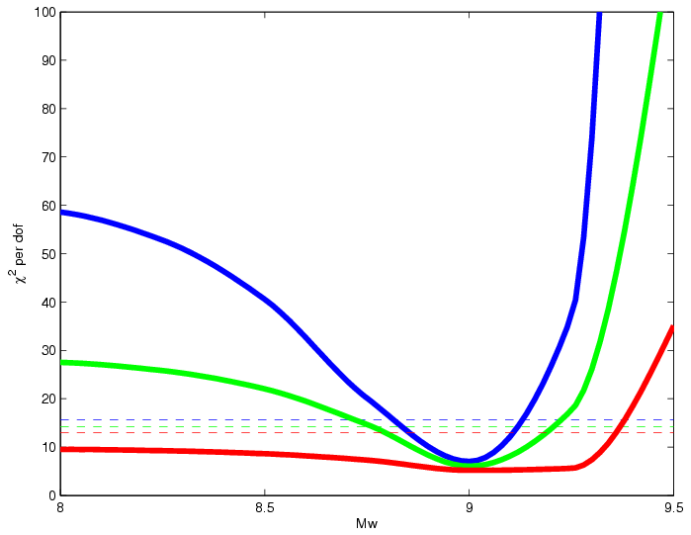

Figure 2. Reduced chi-square χ_v^2 summarizing the misfit of displacements from each model to displacements rapidly determined with GPS, as a function of M_w. Three cases are shown: all stations (blue), all except SAMP (green), and all except SAMP and NTUS (red). The dashed lines indicate 95% confidence intervals for each of the three cases. The smallest misfit using all stations (χ_v^2=7.0) has L=1000 km and M_w 9.0.

We then compared the observed static displacements to those predicted from a suite of physically realistic rupture models, which could in principle be calculated and stored before the earthquake. These models consider different rupture lengths in increments of 200 km. The down-dip width of each segment assumes a 15° dip and that the earthquake slips from the surface to a fixed depth of 40 km (the global average [*Tichelaar and Ruff*, 1993]). We calculated for each rupture length an average slip (over the entire rupture) based on M_w of 8.0–9.5 (in increments of 0.25) using relationships [*Geller*, 1976] between fault length (along-strike dimension), width (downdip dimension), amount of slip, and M_w. The predicted static displacements were then calculated for 105 different cases having anywhere from 1–8 rupture segments modeled as dislocations in a layered spherical Earth [*Pollitz*, 1996].

We applied a fingerprint approach to estimate the magnitude of the earthquake directly from the GPS time series, making use of the fact that for a given fault geometry, the spatial pattern or fingerprint of the displacement depends only on the rupture length, whereas the average slip (hence M_w) simply scales the displacement pattern. The special case of an earthquake model with constant unit slip (1-m) is called a fingerprint model. For each of 15 fingerprint models (of varying rupture lengths), the corresponding magnitude was determined by a least squares fit of the displacement pattern to the GPS time series. Statistics including the variance explained by the fitted predictions, and an *F* test, were used to assess the range of rupture lengths that best fit the data. Using data with a 15-min deadline, we estimate M_w 9.0 for the preferred range of northward-propagating ruptures ranging from 400–1200 km. This estimate depends only weakly on assumed fault length, but ruptures to the south are clearly not preferred.

To assess the statistical significance of M_w 9.0 and its sensitivity to near- and far-field stations, we computed the goodness of fit χ_v^2 for the entire variety of northward rupturing models with a range of M_w 8.0–9.5 (Fig. 2). The preferred rupture length is 1000 km. The best-fitting models have M_w 9.0 even if the near-field sites SAMP and NTUS are excluded. However, the near-field sites are required to reduce the range of admissible magnitudes. The mid-field sites alone strongly constrain the high end of the magnitude scale, but at least one near-field site is required to constrain the low end. The minimum χ_v^2=7.0 is significantly greater than one, presumably due to ground shaking, the long duration (>500 s) of the source [*Vigny et al.*, 2005; *Ishii et al.*, 2005], residual multipath error, and the simplicity of the earthquake models. We therefore used the *F* statistic to reject models that do not fit the data as well as the best fitting model. When both near-field stations are included, the 95% confidence interval is M_w 8.82–9.13. We tested the sensitivity of our modeling to the dip by assuming 10°, 15°, and 20° dips, resulting in additional uncertainties of M_w 0.1–0.2. As a final check, hypothetical scenarios involving strike slip and normal faulting are easily dismissed by *F* tests. We can therefore only accept megathrust models in the range M_w 8.7–9.3, with the most-probable magnitudes M_w 8.9–9.1.

To assess the accuracy of our rapid, best-fitting earthquake model, we compared its predictions with previously published displacements. The RMS

differences in displacement range from 2.5–4.1 mm, which is at the same level of agreement as between the published displacements themselves, indicating that our rapidly estimated model is accurate at this level. Thus a rapid analysis of the existing GPS network can estimate M_w accurately and provide information on the direction and length of rupture propagation, all of which are important for assessing the potential for an open ocean tsunami.

To assess robustness with respect to false alarms, we applied the above procedure to 90 independent sets of data for the day preceding the event. The maximum magnitude estimate in 3 cases was M_w 7.75, well below the threshold for oceanwide tsunamigenesis. False alarms could be further suppressed if the GPS inversion for the earthquake source were only initiated upon seismic triggering above a nominal magnitude threshold.

5. Conclusions

We have shown that the magnitude, mechanism, and spatial extent of rupturing of the 26 December 2004 Sumatra earthquake can be accurately determined using only 15 min of GPS data following earthquake initiation, using publicly available data from existing GPS networks. Most importantly, the GPS method would have clearly ruled out the earliest misleading indications from seismology that there was little danger of a major oceanwide tsunami.

By implementing the GPS displacement method as an operational real-time system, GPS could be incorporated into tsunami warning systems. Sensor networks for tsunami warning systems currently include seismometers and deep ocean pressure recorders that provide real-time data on earthquakes and resulting tsunamis to warning centers, which assess the possible threat and alert emergency managers who advise the public [*Weinstein et al.*, 2005]. The seismic data are important for the rapid detection and location of potentially significant events. GPS data could then be used to rapidly model the earthquake and thus initialize parameters for real-time modeling of tsunami generation. The tsunami models could then be validated and further constrained using ocean sensor data. Thus seismic, geodetic, and oceanic data could be truly integrated in tsunami warning systems. Suitable integrative systems are currently being developed [e.g., *Titov et al.*, 2005].

Our results show greatly enhanced sensitivity to the magnitude of great earthquakes where the global IGS network is augmented by GPS stations in the near field, indicating the advantage of having real-time GPS networks near oceanic subduction zones. Fortunately many such networks exist, or are being planned, and so could be upgraded with real-time communications and incorporated into tsunami warning systems.

Our conclusions are restricted to the problem of identifying submarine earthquakes of such great magnitude (typically $M_w > 8.5$) that they could be capable of generating a major oceanwide tsunami. Local tsunamis are problematic because of the time constraints and sensitivity to local details of the source, bathymetry, coastlines, and resonance effects [*Titov et al.*, 2005]. It should be noted that earthquakes of $M_w > 8.5$ do not always generate destructive oceanwide tsunamis (e.g., 28 March 2005 Nias M_w 8.7 earthquake). This problem, and the more general one of predicting tsunami wave heights, can be addressed by real-time tsunami models that are initialized by earthquake source parameters. The critical parameters for far-field prediction are the seismic moment and the (extended) location of the source [*Titov et al.*, 2005], which our method readily supplies.

Acknowledgments. We thank the International GNSS Service and Bakosurtanal, Indonesia for making GPS data publicly available. Data were processed using GIPSY-OASIS II by the Jet Propulsion Laboratory. This work was supported in part by grants from NASA Interdisciplinary Science and NASA Solid Earth and Natural Hazards. We thank C. Vigny and S. Weinstein for helpful reviews.

References

Banerjee, P., F. F. Pollitz, and R. Burgmann (2005), The size and duration of the Sumatra-Andaman earthquake from far-field static offsets, *Science, 308*, 1769-1772.

Bierman, G. J. (1977), *Factorization Methods for Discrete Sequential Estimation*, Academic Press, San Diego, Calif.

Blewitt G., M. B. Heflin, K. J. Hurst, D. C. Jefferson, F. H. Webb, and J. F. Zumberge (1993), Absolute far-field displacements from the 28 June 1992 Landers earthquake sequence, *Nature, 361*, 340-342.

Bock Y., D. C. Agnew, P. Fang, J. F. Genrich, B. H. Hager, T. A. Herring, K. W. Hudnut, R. W. King, S. Larsen, J. B. minter, K. Stark, S. Wdowinski and F. K. Wyatt (1993), Detection of crustal deformation from the

Landers earthquake sequence using continuous geodetic measurements, *Nature, 361*, 337-340.

Choi, K., A. Bilich, K. Larson, and P. Axelrad (2004), Modified sidereal filtering: Implications for high-rate GPS positioning, *Geophys. Res. Lett., 31*, L22608, doi:10.1029/2004GL021621.

Geller, R.J. (1976), Scaling relations for earthquake source parameters and magnitudes, *Bull. Seismol. Soc. Am., 66*, 1501-1523 (1976).

Genrich, J. F. and Y. Bock (1992), Rapid resolution of crustal motion at short ranges with the Global Positioning System, *Journ. Geophys. Res., 97*, 3261-3269.

Gudmundsson, O. and M. Sambridge (1998), A regionalized upper mantle (RUM) seismic model, *J. Geophys. Res., 103*, 7121-7136.

Kreemer, C., G. Blewitt, W. C. Hammond, and H.-P. Plag (2006), Global deformation from the great 2004 Sumatra-Andaman earthquake observed by GPS: Implications for rupture process and global reference frame, *Earth Planets and Space, 58*, 141-148.

Hanks, T.C., and H. Kanamori (1979), A moment magnitude scale, *J. Geophys. Res., 84*, 2348-2350.

Ishii, M., P. M. Shearer, H. Houston, J. E. Vidale (2005), Extent, duration and speed of the 2004 Sumatra-Andaman earthquake imaged by the Hi-Net array, *Nature, 435*, 933-936.

Kerr, R. A. (2005), Failure to gauge the quake crippled the warning effort, *Science, 307*, 201.

Menke W. and V. Levin, (2005), A strategy to rapidly determine the magnitude of great earthquakes, *Eos Trans. AGU, 86*, 185 and 189.

Okal, E. A., and J. Talandier (1989), Mm: A variable period mantle magnitude, *J. Geophys. Res., 94*, 4169-4193.

Park, J. *et al.* (2005), Earth's free oscillations excited by the 26 December 2004 Sumatra-Andaman earthquake, *Science, 308*, 1139-1144.

Pollitz, F. F. (1996), Coseismic deformation from earthquake faulting on a layered spherical Earth, *Geophys. J. Int., 125*, 1-14.

Stein, S. and E. A. Okal (2005), Speed and size of the Sumatra earthquake, *Nature 434*, 581-582.

Tichelaar, B.W. and L.J. Ruff, (1993), Depth of seismic coupling along subduction zones, *J. Geophys. Res., 98*, 2017- 2037.

Titov, V.V., F.I. González, E.N. Bernard, M.C. Eble, H.O. Mofjeld, J.C. Newman, and A.J. Venturato (2005), Real-time tsunami forecasting: challenges and solutions, *Natural Hazards 35*, 41-58.

Tsai, V. C., M. Nettles, G. Ekström, and A. M. Dziewonski (2005), Multiple CMT source analysis of the 2004 Sumatra earthquake, *Geophys. Res. Lett., 32*, 10.1029/2005GL023813.

Tsuboi, S., K. Abe, K. Takano, Y. Yamanaka (1995), *Bull. Seismol. Soc. Am. 85*, 606-613.

Vigny C., W. J. F. Simons, S. Abu, R. Bamphenyu, C. Satirapod, N. Choosakul, C. Subarya, A. Socquet, K. Omar, H. Z. Abidin, and B. A. C. Ambrosius (2005), Insight into the 2004 Sumatra-Andaman earthquake from GPS measurements in Southeast Asia, *Nature, 436*, 201-206.

Weinstein, S. A. and E. A. Okal (2005), The mantle magnitude Mm and the slowness parameter θ: Five years of real-time use in the context of tsunami warning, *Bull. Seismol. Soc. Am. 95*, 779-799.

Weinstein, S. A., C. McCreery, B. Hirshorn, and P. Whitmore (2005), Comment on "A strategy to rapidly determine the magnitude of great earthquakes" by Menke W. & Levin V., *Eos Trans. AGU, 86*, 263.

G. Blewitt, C. Kreemer, W.C. Hammond, and H.-P. Plag, University of Nevada, 1664 N. Virginia St., MS 178, Reno, NV 89557, USA (gblewitt@unr.edu)

S. Stein and E. Okal, Department of Geological Sciences, Northwestern University, Evanston, IL 60208, USA (seth@earth.northwestern.edu)